Biosorption of mercury by Macrocystis pyrifera and Undaria pinnatifida: Influence of zinc, cadmium and nickel

Josefina Plaza, Marisa Viera, Edgardo Donati, Guibal Eric

Biosorption of mercury by *Macrocystis pyrifera* and *Undaria pinnatifida*: Influence of zinc, cadmium and nickel

Josefina Plaza[1,2], Marisa Viera[1], Edgardo Donati[1], Eric Guibal[2,*]

1. Centro de Investigación y Desarrollo en Fermentaciones Industriales, CINDEFI (CCT La Plata-CONICET, UNLP), Facultad de Ciencias Exactas, 50 y 115, (1900) La Plata, Argentina. E-mail: joplaca@hotmail.com

2. Ecole des Mines d'Alès, Laboratoire Génie de l'Environnement Industriel, 6, avenue de Clavières, F-30319 Alès cedex, France

Abstract

This study investigated the adsorption of Hg(II) on *Macrocystis pyrifera* and *Undaria pinnatifida* in monometallic system in the presence of Zn(II), Cd(II) and Ni(II). The two biosorbents reached the same maximum sorption capacity (q_m = 0.8 mmol/g) for mercury. *U. pinnatifida* showed a greater affinity (given by the coefficient *b* of the Langmuir equation) for mercury compared to *M. pyrifera* (4.4 versus 2.7 L/mmol). Mercury uptake was significantly reduced (by more than 50%) in the presence of competitor heavy metals such as Zn(II), Cd(II) and Ni(II). Samples analysis using an environmental scanning electron microscopy equipped with an energy dispersive X-ray microanalysis showed that mercury was heterogeneously adsorbed on the surface of both biomaterials, while the other heavy metals were homogeneous distributed. The analysis of biosorbents by Fourier transform infrared spectrometry indicated that Hg(II) binding occurred on S=O (sulfonate) and N–H (amine) functional groups.

Key words: mercury; isotherm; sorption; *M. pyrifera*; *U. pinnatifida*; ESEM-EDX; FT-IR spectrometry

Introduction

Mercury is one of the most severe environmental pollutants due to its high toxicity, readily uptake by biota, especially its organic forms, and its subsequent accumulation in the food chain. The use of mercury in industrial processes is progressively being reduced. However, mercury is still used in artisanal mining, batteries and medical devices, causing serious hazards for the environment. The cycle of mercury may comprise elemental form (liquid mercury), ionic forms and organic forms (methyl mercury). The conversion of mercury (in the liquid form) in methyl mercury in water, soil and sediments induces its dispersion and the subsequent contamination of water bodies and biosphere. Methyl mercury is one of the most dangerous forms for entering the food chain. The tragedy of Minamata (Japan) is a lighting example of the mercury transfer through the accumulation in fish that caused serious health problems for fishermen in this area. Mercury poisoning causes a disease called hydrargyria affecting the nervous system, brain, lungs and kidney (Graeme and Pollack, 1998).

Several techniques can be used for the recovery of mercury from dilute solutions, such as chemical precipitation and filtration, chemical oxidation or reduction, electrochemical treatment, reverse osmosis, ion exchange, evaporation and adsorption (Volesky, 2003). However, these processes frequently face several problems for reaching legal discharge levels or for being competitive (especially for low-concentration effluents). For these reasons alternative processes have been investigated. One of them is biosorption that uses materials of biological origin for the sorption of dissolved contaminants. Diverse biological materials (bacteria, algae, fungi, sub- products of food industries) and their sub-products (alginate, chitosan) exhibit interesting metal adsorption capacities (Guibal, 2004). Besides, some of them are easily available in large quantities at low cost and they can be also reused (Bailey et al., 1999; Tsezos, 2001). The use of non-living biomass represents an advantage since it is easier to handle than living biomass, which requires maintaining viable cell conditions.

Mechanisms such as complexation, ion exchange and precipitation may be involved in metal biosorption and also they can simultaneously occur due to the co-existence of different reactive groups on the biomass. The contribution of these different mechanisms to metal sorption may depend on the type of the metals and their speciation. Amine, carboxylic, phosphate, sulphydryl groups are frequently

* Corresponding author. E-mail: Eric.Guibal@mines-ales.fr

identified as the main reactive groups responsible for metal binding. Algae have been widely studied for metal biosorption (Murphy et al., 2008). Brown algae have been especially identified as good sorbents for metal uptake (Romera et al., 2007). *Macrocystis pyrifera* and *Undaria pinnatifida* are two marine brown macroalgae frequently found in the south coast of Atlantic Ocean.

In this work, *M. pyrifera* and *U. pinnatifida* have been tested for mercury removal. Brunauer, Emmett and Teller (BET) multilayer adsorption isotherm, Fourier transform infrared spectrometry (FT-IR) and environmental scanning electron microscopy equipped with an energy dispersive X-ray microanalysis (ESEM-EDX) analyses were used for characterizing the biosorbents and the sorption mechanisms. In addition, sorption studies were performed for determining the impact of pH, sorption isotherms, and the influence of competitor metal ions.

1 Materials and methods

1.1 Biological material

M. pyrifera and *U. pinnatifida* are brown algae belonging to the Phaeophyta class and the Laminariales order. Both were collected on the coast in Bahía de Camarones and Golfo Nuevo (Patagonia, Argentina). Algae biomass was ground and sieved and the particle size fraction 10–16 mesh (i.e., 1.18–2.00 mm) was retained for sorption experiments. Biomass was washed several times with distilled water until obtaining an electrical conductivity less than 1 mS/cm and dried in an oven at 50°C for 48 hr. Biomass was treated for 24 hr with 0.2 mol/L $CaCl_2$ solution at pH 5.0. Then, the biomass was repeatedly washed with distilled water. Finally, the biosorbents were dried in an oven at 50°C for 48 hr and stored in desiccators.

1.2 Kinetic studies

The solutions at initial concentration of 50 mg/L were prepared by dilution of the stock solution (1000 mg/L Hg(II)). pH was controlled to different initial values (i.e., 3.0, 4.0, 5.0 and 6.0). The sorbent dosage was fixed to 1 g/L. The flasks were placed on a magnetic plate and kept stirring at 200 r/min and 20°C. Samples were collected and filtrated at different time intervals for 72 hr. The residual concentration was analyzed by inductively coupled plasma atomic emission spectrometry (ICP-AES Activa-M, Jobin Yvon, Longjumeau, France). To study the effect of other heavy metals on the kinetics of mercury adsorption, Hg(II)-Zn(II), Hg(II)-Cd(II), Hg(II)-Ni(II) binary solutions were prepared at pH 5.0. The final concentration of each metal was 0.25 mmol/L. Other experimental conditions (temperature, sorbent dosage, agitation speed) were the same as those applied for mono-component solutions.

All the experiments were carried out in duplicate. The amount of metal adsorbed was calculated by the mass balance equation:

$$q = \frac{V(C_\mathrm{i} - C_\mathrm{f})}{m} \tag{1}$$

where, q (mg/g or mmol/g) is the solute uptake; C_i (mg/L or mmol/L) and C_f (mg/L or mmol/L) are the initial and final solute concentrations in solution, respectively; V (L) is solution volume and m (g, dry weight basis) is the mass of biosorbent.

Sorption kinetics was analyzed using pseudo-first and, second order rate equations. The reaction rate equations were initially designed for describing chemical reactions in homogeneous systems as pseudo first-order rate equation (PFORE) (Liu and Liu, 2008):

$$\frac{\mathrm{d}q(t)}{\mathrm{d}t} = k_1(q_\mathrm{eq} - q(t)) \tag{2}$$

and after integration (with $q(0) = 0$):

$$\ln\left(1 - \frac{q(t)}{q_\mathrm{eq}}\right) = -k_1 t \tag{3}$$

where, q_eq (mg/g) is the sorption capacity at equilibrium (experimental value), k_1 (1/min) is the pseudo-first order rate constant.

Pseudo-second order rate equation (PSORE) (Ho, 2006):

$$\frac{\mathrm{d}q(t)}{\mathrm{d}t} = k_2(q_\mathrm{eq} - q(t))^2 \tag{4}$$

and after integration (with $q(0) = 0$):

$$q(t) = \frac{q_\mathrm{eq}^2 k_2 t}{1 + q_\mathrm{eq} k_2 t} \tag{5}$$

After linearization:

$$\frac{t}{q(t)} = \frac{1}{k_2 q_\mathrm{eq}^2} + \frac{1}{q_\mathrm{eq}} t \tag{6}$$

where, q_eq (mg/g) is the sorption capacity at equilibrium (calculated value from experimental data), k_2 (g/(mg·min)) is the pseudo-second order rate constant.

1.3 Adsorption isotherms

Mercury sorption isotherms were obtained by mixing 0.1 g of biomass with 100 mL of solution (with initial concentration varying between 10 and 400 mg Hg/L; i.e., 0.05–2.0 mmol/L) for 24 hr at 20°C with a rotating shaker (agitation speed: 150 r/min). The initial pH value of each solution was set at 5.0. The contact time was selected on the basis of kinetic studies. After 24 hr of contact the solution was filtrated and the residual concentration was determined by ICP-AES. The results were adjusted to the Langmuir and Freundlich models.

The Langmuir model suggests monolayer sorption on a homogeneous surface without interaction between sorbed molecules. It is described by Eq. (7):

$$q_\mathrm{e} = \frac{b q_\mathrm{m} C_\mathrm{e}}{1 + b C_\mathrm{e}} \tag{7}$$

where, q_e (mmol/g) is the metal uptake at equilibrium; q_m (mmol/g) is the maximum Langmuir uptake; C_e (mmol/L) is the final concentration at equilibrium; b (L/mmol) is the Langmuir affinity constant. The parameters of the model were determined after linearization of Eq. (7) (i.e., C_e/q_e vs. C_e) and linear regression.

The Freundlich model proposes a monolayer sorption with heterogeneous energetic distribution of active sites, accompanied by interactions between sorbed molecules. The Freundlich model is described by Eq. (8):

$$q_e = K_f C_e^{1/n} \tag{8}$$

where, K_f is a constant relating the biosorption capacity and $1/n$ is an empirical parameter relating the biosorption intensity, which varies with the heterogeneity of the material. The parameters were obtained by linear regression after linearization ($\ln q_e$ vs. $\ln C_e$).

To study the influence of different heavy metals (i.e., Zn(II), Cd(II) and Ni(II)) on mercury adsorption, in binary component solutions, the initial concentrations each metal were varied simultaneously from 0.05 to 1 mmol/L. A given amount (i.e., 0.1 g) of biomass was added to 100 mL of each mixed solution in 150 mL plastic bottles. The bottles were kept stirring at 150 r/min and 20°C for 24 hr.

The uptake of mercury in the presence of other metal cations was represented using the Eq. (9). The sorption capacity was plotted in function of residual concentrations of both mercury and the alternate metal. This model is used for describing a competitive inhibition in enzyme kinetics studies (Chong and Volesky, 1995):

$$q_{M_1} = \frac{(q_m/K_1)\, C_{fM_1}}{1 + (1/K_1) C_{fM_1} + (1/K_2)\, C_{fM_2}} \tag{9}$$

where, q_{M1} (mmol/g) is the metal 1 (i.e., mercury) uptake at equilibrium; q_m (mmol/g) is the maximum binary Langmuir-type uptake for metal 1; C_{fM1} (mmol/L) and C_{fM2} (mmol/L) are the final concentrations for metal 1 and metal 2 at equilibrium, respectively; K_1 (mmol/L) and K_2 (mmol/L) are the inverse binary Langmuir-type affinity constant.

1.4 ESEM-EDX, FT-IR analysis and BET surface area

After metal sorption, biosorbents were recovered, washed three times with demineralized water and dried in an oven at 50°C for 24 hr. Samples were examined using an Environmental Scanning Electron Microscopy (ESEM) (Quanta FEG, FEM, USA), equipped with the OXFORD Inca 350 Energy Dispersive X-ray microanalysis (EDX) system. FT-IR analyses were performed on a FT-IR spectrometer (PerkinElmer, USA) using KBr pellets (the fraction of sample was about 0.1% in weight). The BET Surface Area was determined on approximately 1 g of biomass using krypton gas and a Coulter SA 3100 equipment (Beckman Coulter, USA). The analysis was performed in triplicates.

2 Results and discussion

2.1 Kinetics of mercury removal

The analysis of uptake kinetics is not only useful for elucidating sorption mechanism and determining the rate-controlling steps (the resistance to film diffusion, to intraparticle diffusion and the chemical reaction rates) but also for evaluating the optimum conditions (including equilibrium time) for batch adsorption experiments (Febrianto et al., 2009). Figure 1 shows Hg(II) sorption kinetics adsorption on *M. pyrifera* and *U. pinnatifida* biosorbents. The plots show that the sorption capacity at equilibrium increased with pH for both *M. pyrifera* and *U. pinnatifida*. The optimum sorption was achieved at pH 6. The time necessary to reach the equilibrium was close to 24 hr for *U. pinnatifida*, while for *M. pyrifera* a slight increase of the sorption capacity was observed after 24 hr of contact, especially at pH 3, where the equilibrium plateau was not identified.

Table 1 shows the results obtained by adjusting the experimental data with the PFORE and PSORE models. The comparison of q (modeled using PFORE and PSORE models) with the experimental value of the sorption capacity at equilibrium and the correlation coefficients shows that the PSORE model better fits experimental data than the PFORE model. According to Deng et al. (2006), the rate limiting step, in this case, may be chemisorption involving valence forces through sharing or exchange of electrons between sorbent and sorbate.

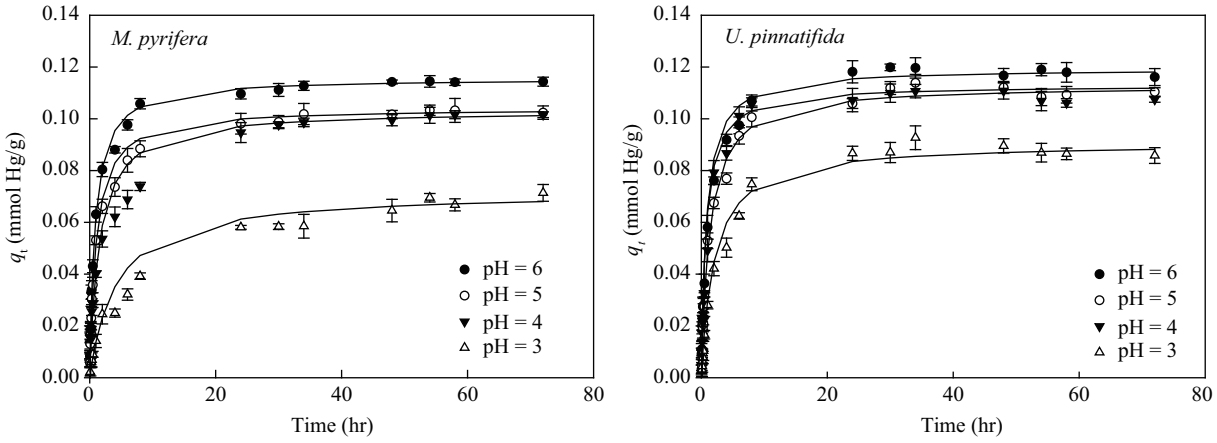

Fig. 1 Adsorption kinetics of Hg(II) at different pH values on *M. pyrifera* (a), and *U. pinnatifida* (b). Bars represent standard deviation for 2 replicates.

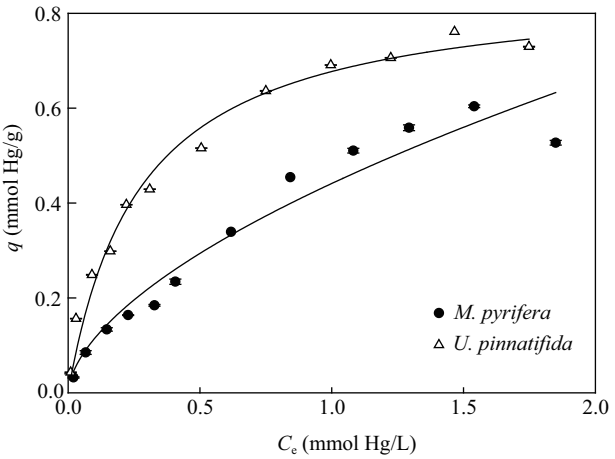

Fig. 2 Adsorption isotherms of Hg(II) by *M. pyrifera* and *U. pinnatifida* as biosorbents at pH 5.0. Bars represent standard deviation for 2 replicates.

2.2 Hg(II) sorption isotherms in mono-component solutions

Sorption isotherms are important to characterize how sorbates can interact with biosorbents. These data are critical to optimize the use of biosorbents (Ho, 2006).

Figure 2 shows the results obtained in the equilibrium experiments for the adsorption of Hg(II) on *M. pyrifera* and *U. pinnatifida* biosorbents.

Table 2 shows the different parameters calculated from the isotherm of Hg(II) using *M. pyrifera* and *U. pinnatifida*, for both the Langmuir and the Freundlich equations. The results obtained from the isotherm for *U. pinnatifida* were well fitted by the Langmuir model (R^2 = 0.99) while the data obtained with *M. pyrifera* adjusted better to Freundlich model (R^2 = 0.98 versus R^2 = 0.91). However, the shape of the sorption isotherms can be characterized by an asymptotic trend that seems more consistent with the Langmuir-type equation than with the power-type equation of the Freundlich equation. The preference for the Freundlich model in the case of *M. pyrifera* can probably be explained by the truncated isotherm: the concentration range was probably not wide enough to reach the saturation plateau. In this case, the sorption isotherm maintains an increasing trend consistent with the power-type shape of the Freundlich equation

The comparison of the isotherms for the two sorbents clearly shows that the same order of magnitude can be reached at saturation (q_m = 0.8 mmol/g or q_m = 160.48 mg/g) while the initial slope, which is representative of the affinity of the sorbent for the sorbate (Sheng et al., 2004), reveals more favorable, in the case of Hg(II), for *U. pinnatifida* than for *M. pyrifera*. Hence the affinity coefficient increases from 2.7 to 4.4 L/mmol for *M. pyrifera* and *U. pinnatifida,* respectively (Table 2). Table 3 summarizes some of the characteristics of the sorption isotherms for Hg(II) using a wide range of synthetic sorbents and biosorbents. A direct comparison is difficult since all these experiments were not performed under same experimental conditions. However, it clearly appears that *M. pyrifera* and *U. pinnatifida* have a higher mercury adsorption capacity than wood-based granular activated carbon, dithiocarbamate-anchored polymer/organosmectite composites, *Ricinus communis* (leaves tree), Poly (c-glutamic acid) (H-form) synthesized from *Bacillus subtilis* and *Azolla filiculoide* (Lloyd-Jones et al., 2004). The two algae used in the present work have practically the same mercury adsorption capacity as other brown algae, specifically *C. baccata* at pH 4.5. But *M. pyrifera* and *U. pinnatifida* have a lower mercury adsorption capacity than Purolite S-920 (containing, isothionium functional groups), Rhom and Haas GT-73 (containing thiol functional groups) (Lloyd-Jones et al., 2004), *Lentinus edodes* (inactive fungal biomass) (Bayramogu and Arıca, 2008) and *C. baccata* at pH 6.0 (Herrero et al., 2005). It must be pointed out that GT-73 is rather unstable in the presence of air due to the oxidation of thiol functional groups and thus the resin must be fully immersed in solution all the time. This is an undesirable feature, despite its higher

Table 1 Kinetic constants for Hg(II) onto *M. pyrifera* and *U. pinnatifida.*

pH	q_{exp}	PFORE model			PSORE model		
		R^2	q (mmol/g)	K_1 (1/min)	R^2	q (mmol/g)	K_2 (g/(mmol·min))
M. pyrifera							
3	0.071	0.95	0.06	9.2×10^{-4}	0.991	0.07	3.30
4	0.10	0.96	0.07	1.6×10^{-3}	0.998	0.10	6.38
5	0.10	0.90	0.06	1.6×10^{-3}	0.999	0.10	9.38
6	0.11	0.93	0.06	1.8×10^{-3}	0.99	0.11	10.18
U. pinnatifida							
3	0.09	0.92	0.07	1.6×10^{-3}	0.998	0.09	5.35
4	0.11	0.90	0.07	2.7×10^{-3}	0.999	0.11	11.51
5	0.11	0.89	0.08	2.0×10^{-3}	0.999	0.11	6.64
6	0.11	0.94	0.08	7.0×10^{-3}	0.999	0.12	10.20

Initial concentration: 0.25 mmol/L; temperature: 20°C; biomass concentration: 0.3 g in 300 mL.

Table 2 Langmuir and Freundlich adsorption constants of Hg(II) on *M. pyrifera* and *U.pinnatifida*

	Langmuir				Freundlich		
	R^2	q_m (mmol/g)	b (L/mmol)	K (mmol/L)	R^2	K_f	Nn
M. pyrifera	0.91	0.82	2.7	0.37	0.98	0.014	1.56
U. pinnatifida	0.99	0.84	4.4	0.22	0.95	0.050	2.08

Table 3 Langmuir parameters obtained for different adsorbents

Adsorbent	pH	q_m (mmol/g)	b (L/mmol)	Reference
Wood based granular activated carbon	4.0	0.1	–	Lloyd-Jones et al., 2004
Purolite S-920 (containing isothionium functional groups)	4.0	1.9	–	
Rhom and Haas GT-73 (containing thiol functional groups)	4.0	3	–	
Azolla filiculoides	4.0	0.2	–	
Lentinus edodes (inactive fungal biomass)	6.0	2	0.7	Bayramoğlu and Arıca, 2008
Poly (c-glutamic acid) (H-form), synthesized from *Bacillus subtilis*	5.0	0.43	24	Inbaraj et al., 2009
Dithiocarbamate-anchored polymer/organosmectite composites	6.0	Hg(II) 0.31, $CH_3Hg(I)$ 0.34, and $C_6H_5Hg(I)$ 0.45		Say et al., 2008
Cystoseria baccata (brown algae)	4.5	0.88	–	Herrero et al., 2005
	6.0	1.59		
Ricinus communis (leaves tree)	5.5	0.18	5.3	Al Rmalli et al., 2008
Penicillium biomass	5.0	1.34	14.04	Svecova et al., 2006
Tolypocladium biomasss	7.0	0.80	80.5	

mercury uptake. The regeneration of Purolite S-920 is not straightforward; this is its major drawback because the recycling and the reuse of resin are important requirements for competitive use of resins (Lloyd-Jones et al., 2004). In spite of its higher mercury adsorption capacity, *Lentinus edodes* (inactive fungal biomass) has a lower mercury affinity coefficient than those determined for *M. pyrifera* and *U. pinnatifida* biomass. In summary, the maximum adsorption capacities of *M. pyrifera* and *U. pinnatifida* are similar to (or even larger than) those obtained with other natural and synthetic materials. Moreover, their relatively high affinity coefficients make these biomaterials suitable for the removal of mercury from wastewater.

2.3 Effect of Cd(II), Zn(II) and Ni(II) on Hg(II) sorption

Figure 3 shows the kinetic profiles for Hg(II) uptake in the presence of competitor metal cations. Table 4 presents the parameters found for the PSORE model in these cases. The presence of the competitor ions modified the adsorption rate of mercury, especially when *M. pyrifera* was used. The highest adsorption constants (K_2) for mercury were obtained in the presence of nickel.

Isotherm experiments in bi-component solutions revealed that the presence of competitor metal cations systematically reduced Hg(II) sorption capacity by three to four times. Table 5 shows the values for the binary Langmuir adsorption parameters found when applying Eq. (9). Some differences were observed regarding the competitor effects of Zn(II), Ni(II) and Cd(II), depending on the type of biosorbent. In the case of *U. pinnatifida*, the sorption capacity decreased from 0.8 mmol Hg/g in mono-component solutions to 0.21 mmol Hg/g, to 0.18 mmol Hg/g and to 0.24 mmol Hg/g in the presence of Zn(II), Cd(II) and Ni(II) respectively. In the case of *M. pyrifera,* the maximum sorption capacity of Hg(II) decreased about ten times: from 0.8 mmol Hg/g (in mono-component system) to 0.08 mmol/g in the presence of Cd(II), and to 0.09 mmol Hg/g in the presence of Ni(II) and Zn(II). The affinity coefficient of *M. pyrifera* and *U. pinnatifida* for Hg(II) increased in the presence of Zn(II), Cd(II) and Ni(II). A higher value of the parameter K determined for a metal in the presence of another metal means that the biosorbent has a higher affinity for the second one (Chong and Volesky, 1995). For example, in the case of *M. pyrifera*, the value of K for Hg(II) decreased from 0.37 for mono-component system to 0.28, 0.02 and 0.05 mmol/L when Zn(II), Cd(II) and Ni(II) are present, respectively in binary component solutions. The same behavior was observed when *U. pinnatifida* was used as biosorbent; in this case, the value of K for Hg(II) decreased from 0.22 for mono-component system to 0.06 mmol/L in presence of Zn(II) and Ni(II) and to 0.02 mmol/L when Cd(II) was the competitor metal in binary component solutions

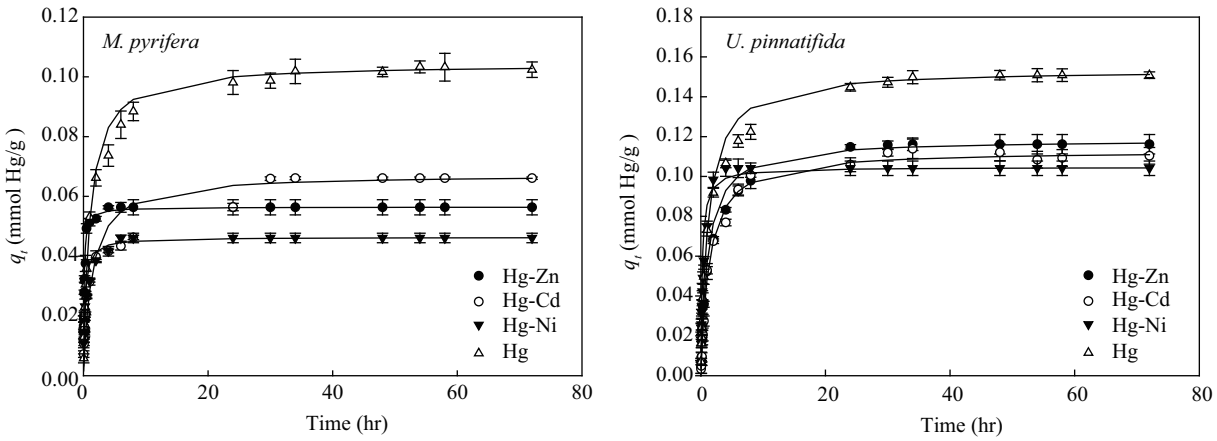

Fig. 3 Adsorption kinetics of Hg(II) in the presence of Zn(II), Cd(II) and Ni(II) on *M. pyrifera* on and *U. pinnatifida*. Bars represent standard deviation for 2 replicates.

Table 4 Pseudo second-order kinetics constants for bimetallic systems using both biosorbents

Biosorbent	Parameter	Hg(II)	Hg(II)-Cd(II)	Hg(II)-Zn(II)	Hg(II)-Ni(II)
M. pyrifera	q (mmol/g)	0.10	0.067	0.056	0.046
	K_2 (g/(mmol·min))	9.38	10.84	10.20	90.96
	R^2	0.9990	0.9970	0.9999	0.9999
U. pinnatifida	q (mmol/g)	0.15	0.11	0.11	0.10
	K_2 (g/(mmol·min))	5.64	6.64	7.68	43.01
	R^2	0.9997	0.9993	0.9998	0.9997

Each metal initial concentration: 0.25 mmol/L; temperature: 20°C; biomass: 0.3 g in 300 mL.

Table 5 Binary-Langmuir adsorption constants of Hg(II)-Zn(II), Hg(II)-Cd(II) and Hg(II)-Ni(II) on *M. pyrifera* and *U. pinnatifida* in bimetallic system

Bimetallic system	*M. pyrifera*				*U. pinnatifida*			
	q_m (mmol/g)	R^2	K_1 (mmol/L)	K_2 (mmol/L)	q_m (mmol/g)	R^2	K_1 (mmol/L)	K_2 (mmol/L)
Hg(II)- Zn(II)	0.48	0.95	0.28	0.03	0.28	0.96	0.06	0.17
Hg(II)- Cd(II)	0.05	0.95	0.02	0.04	0.12	0.96	0.02	0.04
Hg(II)- Ni(II)	0.05	0.98	0.05	0.11	0.18	0.97	0.06	0.30

(Table 5). According to these results mercury adsorption on *M. pyrifera* and *U. pinnatifida* is affected by divalent cations in the following order: Cd(II) ⩾ Ni(II) > Zn(II). These results suggest that *M. pyrifera* and *U. pinnatifida* have a higher affinity for Hg(II) than for Zn(II), Cd(II) and Ni(II).

Other researchers found similar trends. For example, Herrero et al. (2005) observed that the uptake of mercury by *C. baccata* remains practically unaffected in the presence of Cd(II), Mg(II), Zn(II), Ca(II), Cu(II) and Pb(II). They explained their results in terms of different chemical speciation of metals at pH 6.0. Metal speciation is a critical parameter for sorption processes. While mercury is largely present as the neutral species $HgCl_2$, the other metals usually appear as divalent ions, M^{2+}, that can interact with algal cell walls mainly through an electrostatic mechanism. This mechanism limits the competition effect for the sorption of neutral species of mercury. In the case of copper sorption on chitosan, Guzman et al. (2003) showed that, besides some parameters directly related to polymer structure; the speciation of the metal remains one of the most important parameters for predicting the optimum conditions for metal sorption. This parameter is frequently underestimated.

Fungal biomass (*Lentinus edodes)* was tested in multicomponent system (Bayramogu and Arica, 2008). The biosorption capacities of live and heat-inactivated fungal pellets in multi-metal ions systems (Hg(II)-Cd(II)-Zn(II)) were evaluated. They found the following order of affinity, Hg(II) > Cd(II) > Zn(II). The differences in the biosorption affinities could be attributed to differences in electrode potential of these ions and their ionic charge and radius. The high Hg(II) adsorption capacity in mono component system and the high affinity of *Lentinus edodes* for Hg(II) even in the presence of different heavy metals can be explained by Hard and Soft Acid Base Principle (HASB principle). Soft ions, such as Hg(II), form strong bonds with high covalent degree with groups containing nitrogen and sulfur atoms such as CN^-, RS^-, SH^-, NH_2, and imidazol (Nieboer and Richardson, 1980; Pearson, 1963; Remacle, 1990; Wang and Chen, 2009). These chemical groups are frequently identified in the cell wall of different biological materials.

2.4 Biosorbent characterization

At the end of the equilibrium experiments, the final pH of the systems was measured. In the case of *M. pyrifera* the pH increased from 5 to 5.5 while the pH decreased to 4.4 in the experiments conducted with *U. pinnatifida*. The pH variation during Hg(II) sorption in the presence of Zn(II), Cd(II),and Ni(II) was comparable to the pH change in monometallic system. The hydrolysis of mercury may be involved in the increase of the pH value. On the opposite hand, the decrease in pH could be attributed to the release of protons from cell walls because of metal sorption (protons are displaced by exchange with metal ions). The difference in pH variation for *M. pyrifera* and *U. pinnatifida* results would indicate that these biosorbents have different active sites on their cell wall and that the mechanisms involved in mercury biosorption are probably different.

To characterize the biosorbent, different techniques were used. The specific surface areas of the biosorbents were obtained by the BET method: 0.3 m^2/g for *U. pinnatifida* and 0.2 m^2/g for *M. pyrifera*. The differences in the specific surface area are not significant.

ESEM-EDX analyses were conducted to allow the morphological and chemical characterization of the samples. ESEM micrographs of *M. pyrifera* and *U. pinnatifida* particles show that the biosorbents have different morphologies. *M. pyrifera* particles (Fig. 4a, c and e) are more irregular than *U. pinnatifida* particles (Fig. 4b and d).

ESEM-EDX spectra reveals the presence of calcium onto the cell walls indicating that the pretreatment with $CaCl_2$ (0.2 mol/L) was effective for both *M. pyrifera* and *U. pinnatifida*. Uneven distribution of mercury was observed on both algae surfaces (Fig. 4a and b). The biomass employed in the bimetallic isotherms Hg(II)-Zn(II), Hg(II)-Cd(II) and Hg(II)-Ni(II) was also characterized by ESEM-EDX analysis (Fig. 4c, d, and e, respectively). This technique also allowed identifying significant differences in the distribution of metals at the biosorbent surface: while,

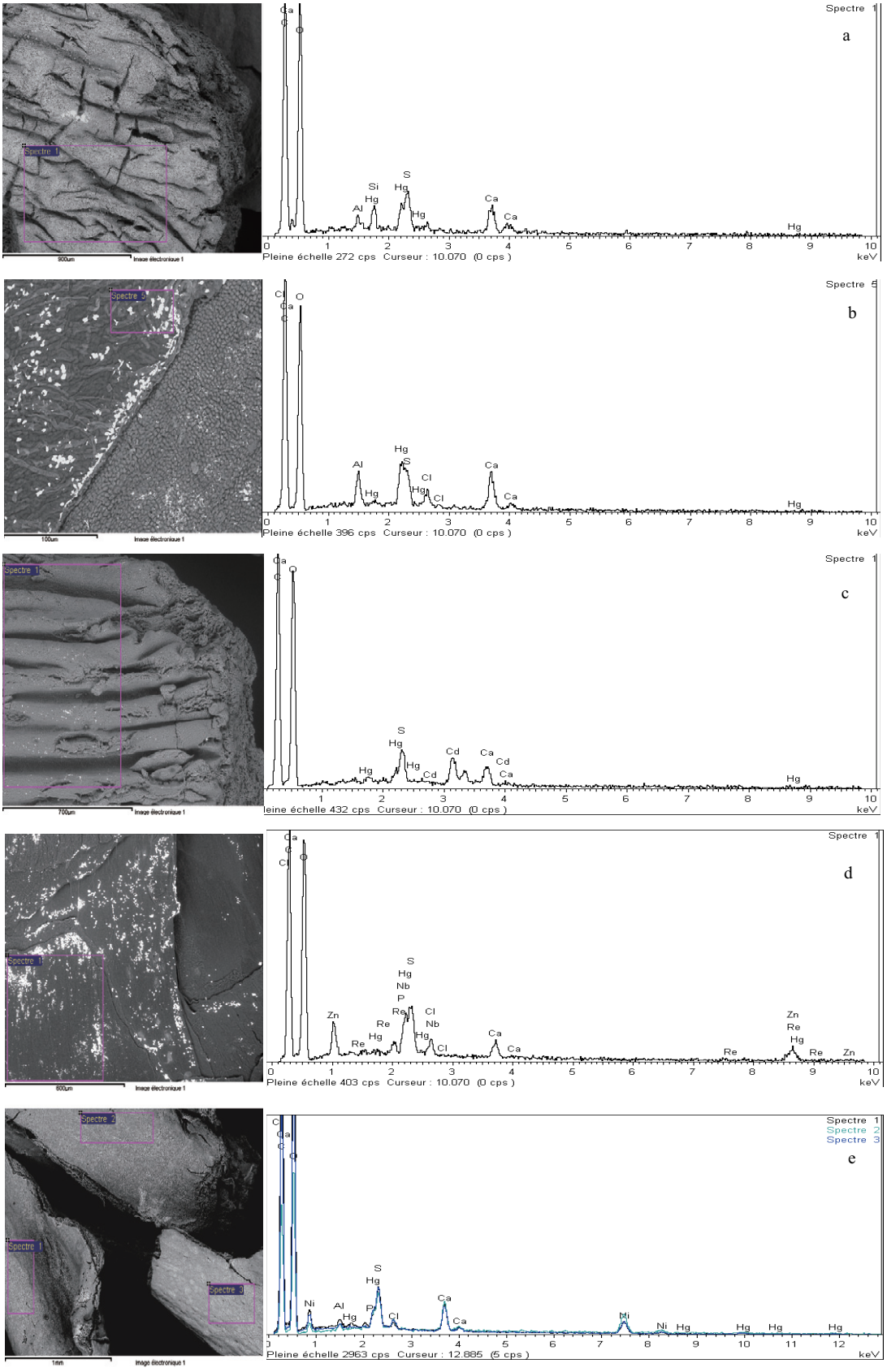

Fig. 4 ESEM-EDX analysis corresponding to: (a) *M. pyrifera* treated with $CaCl_2$ loaded with Hg(II); (b) *U. pinnatifida* treated with $CaCl_2$ loaded with Hg(II); (c) *M. pyrifera* loaded with Hg(II) and Cd(II); (d) *U. pinnatifida* loaded with Hg(II) and Zn(II); (e) *M. pyrifera* loaded with Hg(II) and Ni(II).

Zn(II), Cd(II), and Ni(II) ions were found uniformely distributed on the algal surfaces, Hg(II) was only detected in aggregates (which can be seen as white dots in the microphotographs of Fig. 4)

To obtain further insight into the modification on the surface of the biomass due to the mercury sorption, FT-IR

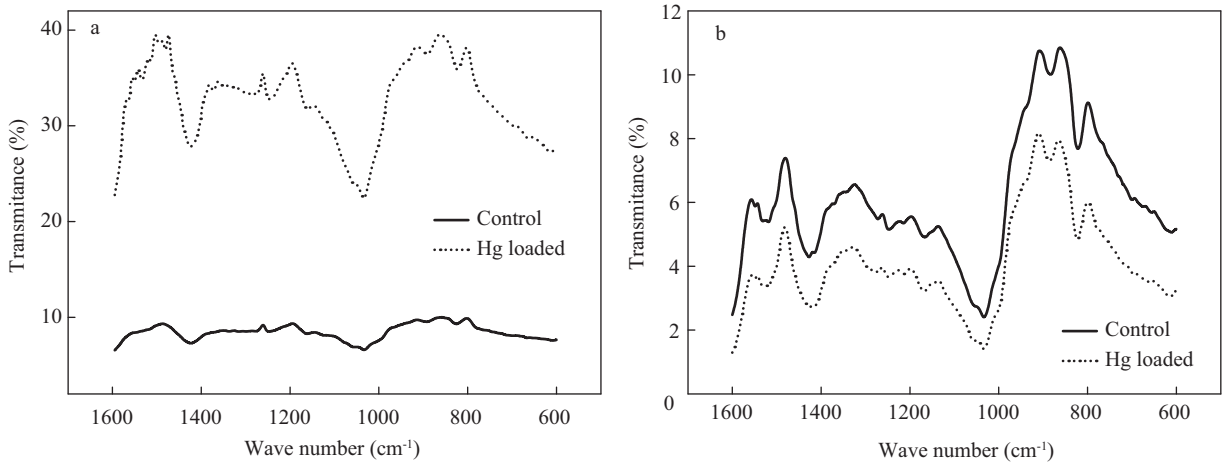

Fig. 5 FT-IR spectra of *M. pyrifera* (a) and *U. pinnatifida* (b).

analysis was performed. Numerous chemical groups have been proposed to be responsible for the biosorption of metals by macroalgae. Carboxylic groups are involved in metal binding reactions in biological materials. Nevertheless, N- and S-containing groups from proteins may also be important for metal ion binding (Yalçin et al., 2010). Their relative importance in metal sorption may depend on factors such as the quantity of sites, their accessibility, chemical state, and affinity between sites and metal (Pavasant et al., 2006). Figure 5 shows the FT-IR spectra corresponding to *M. pyrifera* and *U. pinnatifida*, respectively, before and after Hg(II) sorption. The presence of amine groups on the cell wall of both biomaterials was confirmed by the presence of the peak at 1619 cm^{-1} (N–H bending) and peaks between 1340–1020 (C–N stretching). The peaks found in the range 700–900 cm^{-1} can be attributed to organic sulfur-bounds (S–O; S–C). The interaction with Hg(II) induced some peak shifts, from 1522 to 1519 cm^{-1} (N–H stretching) and 1245 to 1250 cm^{-1} (C–O alcohol or carboxylic acid stretching). In the case of *M. pyrifera* (Fig. 5a), the main difference between the control and the loaded biomass spectra consists in the presence of peaks attributed to C–H bound (885 cm^{-1}) in the loaded biomass. The spectra of control and Hg(II)-loaded biomass of *U. pinnatifida* are very similar (Fig. 5b) and exhibit a higher diversity of active sites than those observed in *M. pyrifera* biomass.

FT-IR studies revealed that the most important chemical groups involved in Hg(II) binding to *U. pinnatifida* and *M. pyrifera* are carboxyl, sulfonate, and amine groups. FT-IR results agree with the HASB principle which indicates that the groups containing nitrogen and sulfur atoms have an important role in Hg(II) adsorption. This could explain the similar adsorption capacities of Hg(II) by both biomaterials.

3 Conclusions

M. pyrifera and *U. pinnatifida* are both brown algae belonging to the same family (Phaeophyta). However they present significant differences in their biosorption properties. The maximum Hg(II) sorption capacity (based on Langmuir model) was 0.82 mmol/g and 0.84 mmol/g for *M. pyrifera* and *U. pinnatifida*, respectively. Although both biomaterials have similar q_m, *U. pinnatifida* has a higher affinity for Hg(II) than that of *M. pyrifera*. The sorption of Hg(II) was significantly affected by the presence of Zn(II), Cd(II), and Ni(II), as reducing mercury uptake up to ten times for *U. pinnatifida* and by less than four times for *M. pyrifera*.

The pH variation during the adsorption experiments depended on the biosorbent: it increased in the case of *M. pyrifera*, and decreased in the case of *U. pinnatifida* in both mono-component solutions and binary component solutions.

The distribution of mercury on the cell wall is concentrated in certain parts, while the sorption of Zn(II), Cd(II) and Ni(II) was homogeneous on the surface of the cell wall as shown by ESEM–EDX analyzes. According to FT-IR analysis and the HASB theory, the affinity for Hg(II) could be related to the presence of amino and sulfur groups at the surface of the biosorbents. These functional groups play an important role in Hg(II) sorption on these algal biomass.

Acknowledgments

Dr. Edgardo Donati and Dr. Marisa Viera are research members of CONICET. This research was supported by ANPCyT (PICT 25300), CONICET (PIP 5147) and by the European Commission through the ALFA program BIO-PROAM (Contract number: AML/190901/06/18414/II-0548-FC-FA).

References

Al Rmalli S W, Dahmani A A, Abuein M M, Gleza A A, 2008. Biosorption of mercury from aqueous solutions by powdered leaves of castor tree (*Ricinus communis* L.). *Journal of Hazardous Materials*, 152(3): 955–959.

Bailey S E, Olin T J, Bricka R M, Adrian D D, 1999. A review of potentially low-cost sorbents for heavy metals. *Water Research*, 33(11): 2469–2479.

Bayramoğu G, Arıca M Y, 2008. Removal of heavy mercury(II), cadmium(II) and zinc(II) metal ions by live and heat

inactivated *Lentinus edodes* pellets. *Chemical Engineering Journal*, 143(1-3): 133–140.

Chong K S, Volesky B, 1995. Description of two-metal biosorption equilibria by Langmuir-type models. *Biotechnology Bioengineering*, 47(4): 451–460.

Deng L P, Su Y Y, Su H, Wang X T, Zhu X B, 2006. Biosorption of copper(II) and lead(II) from aqueous solutions by non-living green algae *Cladophora fascicularis*: equilibrium, kinetics and environmental effects. *Adsorption*, 12(4): 267–277.

El-Sikaily A, El Nemr A, Khaled A, Abdelwehab O, 2007. Removal of toxic chromium from wastewater using green alga *Ulva lactuca* and its activated carbon. *Journal of Hazardous Materials*, 148(1-2): 216–228.

Febrianto J, Kosasih A N, Sunarso J, Ju Y H, Indraswati N, Ismadji S, 2009. Equilibrium and kinetic studies in adsorption of heavy metals using biosorbent: a summary of recent studies. *Journal Hazardous Materials*, 162(2-3): 616–645.

Graeme K A, Pollack C V, 1998. Heavy metal toxicity, part 1: arsenic and mercury. *The Journal Emergency Medicine*, 16(1): 45–56.

Guibal E, 2004. Interactions of metal ions with chitosan-based sorbents: a review. *Separation and Purification Technology*, 38(1): 43–74.

Guzman J, Saucedo I, Revilla J, Navarro R, Guibal E, 2003. Copper sorption by chitosan in the presence of citrate ions: influence of metal speciation on sorption mechanism and uptake capacities. *International Journal of Biological Macromolecules*, 33(1-3): 57–65.

Herrero R, Lodeiro P, Rey-Castro C, Vilariño T, Sastre de Vicente M E, 2005. Removal of inorganic mercury from aqueous solutions by biomass of marine macroalga *Cystoseira baccata*. *Water Research*, 39(14): 3199–3210.

Ho Y S, 2006. Second-order kinetic model for sorption of cadmium onto tree fern: a comparison of linear and non – linear methods. *Water Research*, 40(1): 119–125.

Inbaraj B S, Wang J S, Lu J F, Siao F Y, Chen B H, 2009. Adsorption of toxic mercury(II) by an extracellular biopolymer poly (γ-glutamic acid). *Bioresource Technology*, 100(1): 200–207.

Liu Y, Liu Y J, 2008. Biosorption isotherms, kinetics and thermodynamics. *Separation and Purification Technology*, 61(3): 229–242.

Lloyd-Jones P J, Rangel-Mendez J R, Streat M, 2004. Mercury sorption from aqueous solution by chelating ion exchange resins, activated carbon and a biosorbent. *Process Safety and Environmental Protection*, 82(4): 301–311.

Martin J P, Cuevas J M, 2006. First record of *Undaria pinnatifida* (Laminariales, Phaeophyta) in Southern Patagonia, Argentina. *Biological Invasions,* 8(6): 1399–1402.

Murphy V, Hughes H, McLoughlin P, 2008. Comparative study of chromium biosorption by red, green and brown seaweed biomass. *Chemosphere*, 70(6): 1128–1134.

Nieboer E, Richardson D H S, 1980. The replacement of the nodescript term 'heavy metals' by a biologically and chemically significant classification of metal ions. *Environmental Pollution Series B, Chemical and Physical*, 1(1): 3–26.

Pavasant P, Apiratikul R, Sungkhum V, Suthiparinyanont P, Wattanachira S, Marhaba T F, 2006. Biosorption of Cu^{2+}, Cd^{2+}, Pb^{2+}, and Zn^{2+} using dried marine green macroalga *Caulerpa lentillifera*. *Bioresource Technology*, 97(18): 2321–2329.

Pearson R G, 1963. Hard and soft acids and bases. *Journal of American Chemical Society*, 85(22): 3533–3539.

Remacle J, 1990. The cell wall and metal binding. In: Biosorption of Heavy Metals (Volesky B, ed.). CRC Press, Boca Raton. 83–92.

Romera E, González F, Ballester A, Blázquez M L, Muñoz J A, 2007. Comparative study of biosorption of heavy metals using different types of algae. *Bioresource Technology*, 98(17): 3344–3353.

Say R, Birlik E, Erdemgil Z, Denizli A, Ersöz A, 2008. Removal of mercury species with dithiocarbamate – anchored polymer/organosmectite composites. *Journal of Hazardous Materials*, 150(3): 560–564.

Sheng P X, Ting Y P, Chen J P, Hong L, 2004. Sorption of lead, cooper, cadmium, zinc, and nickel by marine biomass: characterization of biosorptive capacity and investigation of mechanisms. *Journal of Colloid and Interface Science*, 275(1): 131–141.

Svecova L, Spanelova M, Kubal M, Guibal E, 2006. Cadmium, lead and mercury biosorption on waste fungal biomass issued from fermentation industry. I. Equilibrium studies. *Separation and Purification Technology*, 52(1): 142–153.

Tsezos M, 2001. Biosorption of metals. The experience accumulated and the outlook for technology development. *Hydrometallurgy*, 59(2-3): 241–243.

Volesky B, 2003. Sorption and Biosorption. B. V. Sorbex. Inc., Montreal-St. Lambert, Quebec, Canada.

Wang J L, Chen C, 2009. Biosorbents for heavy metals removal and their future. *Biotechnology Advances*, 27(2): 195–226.

Yalçın E, Çavuşoğlu K, Kınalıoğlu K, 2010. Biosorption of Cu^{2+} and Zn^{2+} by raw and autoclaved *Rocella phycopsis. Journal of Environmental Sciences*, 22(3): 367–373.